*Inorg. Chem.* **2002**, *41*, 6553–6559


# Pd(0) and Pt(0) Metallocryptands Encapsulating a Spinning Mercurous Dimer

**Vincent J. Catalano* and Mark A. Malwitz**

*Department of Chemistry, University of Nevada, Reno, Nevada 89557*

**Bruce C. Noll**

*Department of Chemistry and Biochemistry, University of Colorado, Boulder, Colorado 80309*

Received July 8, 2002

The deep-red, air-stable complexes $[Pt_2Hg_2(P_2phen)_3](PF_6)_2$, **1**, or $[Pd_2Hg_2(P_2phen)_3](PF_6)_2$, **2**, ($P_2$phen is 2,9-bis-(diphenylphosphino)-1,10-phenanthroline) are most conveniently prepared by the stoichiometric reaction of either $Pt(dba)_2$ or $Pd_2(dba)_3{\cdot}CHCl_3$ (dba is dibenzylideneacetone) with $P_2$phen and a single drop of elemental mercury in refluxing dichloromethane under an atmosphere of nitrogen. The $^{31}P\{^1H\}$ NMR spectrum ($CD_3CN$) of **1** shows a single sharp resonance at 43.1 ppm for the phosphorus atoms of the $P_2$phen ligand with both $^{195}Pt$ ($^1J_{P-Pt} = 4350$ Hz) and $^{199}Hg$ ($^2J_{P-Hg} = 620$ Hz) satellites indicating the $Hg_2^{2+}$ unit is dynamic. Compound **2** has a similar resonance at 44.9 ppm with $^{199}Hg$ satellites ($^2J_{P-Hg} = 638$ Hz). The $^{199}Hg$ NMR ($CD_2Cl_2$, vs $Hg(OAc)_2$) spectrum of **2** shows a heptet pattern at 833 ppm while for **1** a heptet superimposed on a doublet of heptets is observed at 770.8 ppm. The $^{195}Pt$ NMR spectrum of **1** displays a quartet at −3071 ppm with $^{199}Hg$ satellites and a $^1J_{Pt-Hg}$ value of 1602 Hz. Characterization of **1** and of $\mathbf{2(BF_4)_2}$ by single-crystal X-ray diffraction studies confirms the metallocryptand structure consisting of three phosphine–imine ligands forming a $D_3$ symmetric cage with a $Hg_2^{2+}$ ion in its center coordinated to two phenanthroline rings with the Hg–Hg bond (**1**, 2.7362(6); $\mathbf{2(BF_4)_2}$, 2.6881(4) Å) oriented perpendicular to the vector between the trigonally coordinated Pt(0) or Pd(0) atoms on each end. The Pt–Hg separations in **1** average 2.8143(6) Å while in $\mathbf{2(BF_4)_2}$ the average Pd–Hg separation is 2.7698(5) Å. Excitation into the low energy excitation bands of **1** (475 nm) and **2** (430 nm) produces weak emissions centered at 593 nm with shoulders at 530 and 654 nm in **1** and centered at 524 nm with a shoulder at 545 nm in **2**.

## Introduction

The investigation of interactions between closed-shell, heavy metal ions or atoms continues to gather increasing attention.[1] Numerous examples of heavy metal ions such as Au(I), Ag(I), Tl(I), or Pb(II) or metal atoms such as Pt(0), Pd(0), or Hg(0) associating with each other or with other similar species have been reported.[2−4] Elucidating the nature of these attractive interactions has been the subject of considerable theoretical effort and only recently has the role of dispersion forces as the primary attractive force in metallophilic attractions been clarified.[5] Additionally, relativistic effects may also play a significant role in aurophilic attractions.[6]

**Scheme 1**

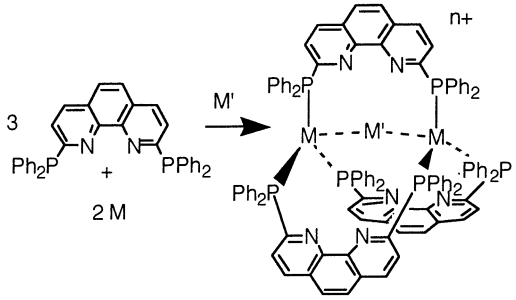


The importance of these noncovalent attractions is clearly demonstrated in our work[7−11] employing metallocryptands as probes of metal−metal interactions (Scheme 1). The internal pockets of these cages are suitably sized to effectively encapsulate metal guests without imposing steric restrictions from the ligands, and by a simple twisting of

* To whom correspondence should be addressed. E-mail: vjc@unr.edu. Fax: (775) 784-6804.

(1) Gade, L. H. *Angew. Chem., Int. Ed.* **2001**, *40*, 3573−3575.
(2) Pyykkö, P. *Chem. Rev.* **1997**, *97*, 597−636.

10.1021/ic020439n CCC: $22.00 
Published on Web 10/05/2002

**Table 1.** Intermetallic Separations and Angles of $[M_2M'(P_2phen)_3]^{n+}$ Metallocryptands

| $d^{10}$ metal, M | guest, M′ | separation, Å | M−M′−M angle, deg | av Δd,[a] Å | ref |
|---|---|---|---|---|---|
| Pd(0) | Pb(II) | 2.7095(6)<br>2.6902(6) | 178.75(1) | −0.121 | 8 |
| Pt(0) | Pb(II) | 2.7469(6)<br>2.7325(6) | 178.75(1) | −0.093 | 8 |
| Pt(0) | Tl(I) | 2.7907(9)<br>2.7919(9) | 175.27(3) | −0.053 | 9 |
| Pd(0) | Tl(I) | 2.7914(6) | 160.62(3) | −0.041 | 9 |
| Au(I) | Hg(0) | 2.7847(4)<br>2.7807(4) | 170.48(1) | +0.007 | 7 |
| Au(I) | Tl(I) | 2.9171(5)<br>2.9109(5) | 174.5(1) | +0.029 | 10 |

[a] Determined as the difference between the metal−metal separation as measured by X-ray crystallography and the predicted single-bond separation taken from a standard source.[27]

the overall helical structure, the intermetallic separations can be varied. For the $P_2$phen-based metallocryptands ($P_2$phen is 2,9-bis(diphenylphosphino)-1,10-phenanthroline), the greatest attraction is observed in the Pd(0)−Pb(II)−Pd(0)[8] system (Table 1) where an attractive ion-induced dipole interaction predominates. The longest metal−metal interaction is observed in the Au(I)−Tl(I)−Au(I)[10] species where the added electrostatic repulsion of the similarly charged metals negates much of the aurophilic attraction of the Tl(I) ion. As expected, the monovalent Tl(I) ion is held less strongly than the isoelectronic, divalent Pb(II) ion in the Pd(0) and Pt(0) metallocryptands, and the Au(I)−Hg(0)−Au(I) species with the polarizable metal in the middle falls intermediate in this series. In all of these complexes, only a single metal atom or ion is encapsulated, and this metal resides in the center of the cavity formed by the three $P_2$phen ligands and does not interact strongly with the phenanthroline nitrogen donor atoms.

The successful encapsulation of Hg(0) into the cavity of the Au(I) metallocryptand[7] led us to investigate whether the isoelectronic Pt(0)−Hg(0)−Pt(0) or Pd(0)−Hg(0)−Pd(0) species could be made. The absence of charge in this molecule would preclude any ion-induced dipole interaction, and any metallophilic attractions would then be purely dispersive in nature. Unfortunately, attempts to produce a Pt(0)−Hg(0)−Pt(0) or Pd(0)−Hg(0)−Pd(0) metallocryptand failed; however, here we report the unexpected redox chemistry of this attempt leading to the first encapsulation of a mercurous dimer ($Hg_2^{2+}$) into a metallocryptand and its unprecedented multimetallic bonding mode.

## Experimental Section

All preparations were carried out under a $N_2$ atmosphere with the use of standard Schlenk techniques. Acetonitrile and dichloromethane were purified by passage through a column of activated alumina using a Grubbs apparatus.[12] Solvents utilized in preparations were deoxygenated by three freeze−pump−thaw cycles prior to use. $P_2$phen,[9] $Pt(dba)_2$,[13] and $Pd_2(dba)_3{\cdot}CHCl_3$[14] were prepared from literature procedures. Where needed, elemental mercury was purified by simple bulb-to-bulb distillation under vacuum prior to use. NMR chemical shift reference materials were the following: $^{199}$Hg, $Hg(OAc)_2$ in $d_6$-DMSO; $^{195}$Pt, $H_2PtCl_6$ in $D_2O$; $^{31}$P, 85% $H_3PO_4$. Cyclic voltammetric experiments were carried out using a BAS CW50 instrument with the following cell configuration: Pt or glassy carbon working electrodes, Pt wire auxiliary electrode, Ag/AgCl reference in a modified Lugin electrode. Solutions were prepared with 0.1 M TBAP as electrolyte in nitrogen-purged MeCN and referenced to internal $Cp_2Fe$. Combustion analysis was carried out by Desert Analytics, Tucson, AZ. UV−vis spectra were obtained using a Hewlett-Packard 8453 diode array spectrometer (1 cm path-length cells). Emission data were recorded using a Spex Fluoromax steady-state fluorometer.

**Preparation of $[Pt_2Hg_2(P_2phen)_3](PF_6)_2$, 1.** Under nitrogen, a 100 mL Schlenk flask was charged with 0.081 g (0.1220 mmol) of $Pt(dba)_2$, 0.100 g (0.1823 mmol) of 2,9-bis(diphenylphosphino)-1,10-phenanthroline ($P_2$phen), and 40 mL of deoxygenated $CH_2Cl_2$. After this mixture was stirred for 10 min, a drop of elemental mercury was added, and the mixture was heated to reflux overnight. The resulting brick-red solution was then opened to air and filtered through Celite, and volatiles were removed with a rotary evaporator. To the remaining red oil was added an excess amount of $NH_4PF_6$ and 20 mL of $CH_3CN$. This mixture was placed in an ultrasonic cleaner for ca. 5 min after which the volatiles were removed. The remaining reddish-brown solid was dissolved in $CH_2Cl_2$ and filtered through Celite. Flash chromatography (alumina, 2.5 cm × 15 cm), eluting first with $CH_2Cl_2$ until yellow dba is removed and then with $CH_3OH$, affords a reddish-brown solid after removal of solvent. Precipitation of the reddish-brown solid by addition of $Et_2O$ to a saturated $CH_2Cl_2$ solution affords 0.106 g (0.0389 mmol) of **1** as a reddish-brown solid (64%). Anal. Calcd ($C_{119}H_{94}Cl_2F_{12}Hg_2N_6P_8Pt_2$): C, 48.51; H, 3.22; N, 2.85. Found: C, 48.98; H, 2.82; N, 3.25. $^1$H NMR (300 MHz, $CD_3CN$, 25 °C): $\delta = 8.41$ (d, $J = 8.06$ Hz), 8.14 (s), 7.60 (d, $J = 8.06$ Hz), 7.32 (m), 6.96 (m), 6.94 (m), 6.72 (m), 6.25 (m), 5.80 (m). $^{31}$P{$^1$H} NMR (121 MHz, $CD_3CN$,


(3) (a) Hamel, A.; Mitzel, N. W.; Schmidbaur, H. *J. Am. Chem. Soc.* **2001**, *123*, 5106−5107. (b) Hayashi, A.; Olmstead, M. M.; Attar, S.; Balch, A. L. *J. Am. Chem. Soc.* **2002**, *124*, 5791−5795. (c) Burini, A.; Bravi, R.; Fackler, J. P., Jr.; Galassi, R.; Grant, T. A.; Omary, M. A.; Pietroni, B. R.; Staples, R. J. *Inorg. Chem.* **2000**, *39*, 3158−3165. (d) Fernández, E. J.; Laguna, A.; López-de-Luzuriaga, J. M.; Monge, M.; Pyykkö, P.; Runeberg, N. *Eur. J. Inorg. Chem.* **2002**, *3*, 750−753. (e) Fernández, E. J.; López-de-Luzuriaga, J. M.; Monge, M.; Olmos, M. E.; Pérez, J.; Laguna, A. *J. Am. Chem. Soc.* **2002**, *124*, 5942−5943. (f) Crespo, O.; Fernández, E. J.; Jones, P. G.; Laguna, A.; López-de-Luzuriaga, J. M.; Mendia, A.; Monge, M.; Olmos, E. *Chem. Commun.* **1998**, 2233−2234. (g) Burini, A.; Fackler, J. P., Jr.; Galassi, R.; Grant, T. A.; Omary, M. A.; Rawashdeh-Omary, M. A.; Pietroni, B. R.; Staples, R. J. *J. Am. Chem. Soc.* **2000**, *122*, 11264−11265.

(4) Catalano, V. J.; Bennett, B. L.; Muratidis, S.; Noll, B. C. *J. Am. Chem. Soc.* **2001**, *123*, 173−174.

(5) (a) Pyykkö, P.; Straka, M. *Phys. Chem. Chem. Phys.* **2000**, *2*, 2489−2493. (b) Runeberg, N.; Schütz, M.; Werner, H.-J. *J. Chem. Phys.* **1999**, *110*, 7210−7215.

(6) (a) Pyykkö, P.; Mendizabal, F. *Inorg. Chem.* **1998**, *37*, 3018−3025. (b) Pyykkö, P.; Mendizabal, F. *Chem.—Eur. J.* **1997**, *3*, 1458−1465. (c) Pyykkö, P.; Runeberg, N.; Mendizabal, F. *Chem.—Eur. J.* **1997**, *3*, 1451−1457.

(7) Catalano, V. J.; Malwitz, M. A.; Noll, B. C. *Chem. Commun.*, **2001**, 581−582.

(8) Catalano, V. J.; Bennett, B. L.; Noll, B. C. *Chem. Commun.* **2000**, 1413−1414.

(9) Catalano, V. J.; Bennett, B. L.; Yson, R.; Noll, B. C. *J. Am. Chem. Soc.*, **2000**, *122*, 10056−10062.

(10) Catalano, V. J.; Bennett, B. L.; Kar, H. M.; Noll, B. C. *J. Am. Chem. Soc.*, **1999**, *121*, 10235−10236.

(11) Catalano, V. J.; Kar, H. M.; Bennett, B. L. *Inorg. Chem.* **2000**, *39*, 121−127.

(12) Pangborn, A. B.; Giardello, M. A.; Grubbs, R. H.; Rosen, R. K.; Timmers, F. J. *Organometallics* **1996**, *15*, 1518−1520.

(13) Cherwinski, W. J.; Johnson, B. F. G.; Lewis, J. *J. Chem. Soc., Dalton Trans.* **1974**, 1405−1409.

(14) Ukai, T.; Kawazura, H.; Ishii, Y.; Bonnet, J. J.; Ibers, J. A. *J. Organomet. Chem.* **1974**, *65*, 253−266.

25 °C): $\delta = 43.1$ (s, $^1J_{P-Pt} = 4350$ Hz, $^2J_{P-Hg} = 620$ Hz). $^{195}$Pt NMR (106.95 MHz, $CD_2Cl_2$, external reference $H_2PtCl_6$ in $D_2O$, 25 °C): $\delta = -3071$ (q, $^1J_{Pt-P} = 4350$ Hz, $^1J_{Pt-Hg} = 1602$ Hz). $^{199}$Hg NMR (89.385 MHz, $CD_2Cl_2$, external reference $Hg(OAc)_2$ in $d_6$-DMSO, 25 °C): $\delta = 770.8$ (hept, $^2J_{Hg-P} = 620$ Hz, dhept, $^1J_{Hg-Pt} = 1602$ Hz).

**Preparation of $[Pd_2Hg_2(P_2phen)_3](PF_6)_2$, 2.** Prepared analogously to **1**. Yield: 61%. $^1$H NMR (300 MHz, $CD_3CN$, 25 °C): $\delta = 8.48$ (d, $J = 8.05$ Hz), 8.15 (s), 7.58 (d, $J = 8.05$ Hz), 7.32 (m), 7.01 (m), 6.94 (m), 6.726 (m), 6.25 (m), 5.79 (m). $^{31}$P{$^1$H} NMR (121 MHz, $CD_3CN$, 25 °C): $\delta = 44.9$ (s, $^2J_{P-Hg} = 638$ Hz). $^{199}$Hg NMR (89.392 MHz, $CD_2Cl_2$, external reference $Hg(OAc)_2$ in $d_6$-DMSO, 25 °C): $\delta = 833$ (hept, $^2J_{Hg-P} = 638$ Hz).

**$[Pd_2Hg_2(P_2phen)_3](BF_4)_2$, 2($BF_4$)$_2$** was prepared quantitatively by metathesis of **2** with excess $NaBF_4$ and crystallized by slow addition of benzene to a 1,2-dichloroethane solution of the complex.

**X-ray Crystallography.** Suitable crystals were coated with light petroleum oil, mounted on a glass fiber, and placed in the nitrogen cold stream of a Siemens SMART diffractometer. Unit cell parameters were determined by least-squares analysis of 9125 reflections with $2.40° < \theta < 31.2°$ for **1** and 7529 reflections with $2.24° < \theta < 27.73°$ for **2**. A total of 99964 reflections were collected in the range $1.77° < \theta < 27.5°$, yielding 24741 unique reflections ($R_{int} = 0.068$) for **1**, while a total of 151998 reflections were collected in the range $1.27° < \theta < 27.5°$, yielding 22568 unique reflections ($R_{int} = 0.105$) for **2**. The data were corrected for absorption and Lorentz and polarization effects. Crystal data are given in Table 3. Scattering factors and corrections for anomalous dispersion were taken from a standard source.[15]

Calculations were performed using the Siemens SHELXTL Version 5.10 system of programs refining on $F^2$. The structures were solved by direct methods. Complexes **1** and **2**($BF_4$)$_2$ crystallize in the monoclinic space group, $P2(1)/n$. Complex **1** crystallizes with the cation, two hexafluorophosphate anions (one is positionally disordered about the fluorine atoms), one 1,2-dichloroethane molecule, and one and one-half benzene solvate molecules. Likewise, **2**($BF_4$)$_2$ crystallizes with the cation, two tetrafluoroborate anions (one is disordered about the fluorine atoms), three-quarters of a 1,2-dichloroethane molecule and one-half of a benzene solvate. There are no unusual contact between these moieties. The refinements of these data were unremarkable. Simple models of the disorder provided satisfactory refinements.

## Results

The deep-red, air-stable complexes $[Pt_2Hg_2(P_2phen)_3](PF_6)_2$, **1**, or $[Pd_2Hg_2(P_2phen)_3](PF_6)_2$, **2**, are most conveniently prepared by the stoichiometric reaction of either $Pt(dba)_2$ or $Pd_2(dba)_3$ (dba is dibenzylideneacetone) with $P_2$phen and a single drop of commercial, triply distilled, elemental mercury in refluxing dichloromethane under an atmosphere of nitrogen. Metathesis with $NH_4PF_6$ produces **1** and **2** in moderate yields. In this method, the necessary redox chemistry to form $Hg_2^{2+}$ likely results from an oxidative addition reaction between the solvent and the zerovalent metal followed by a second redox process with Hg(0) to generate the mercurous dimer. Surprisingly, the anaerobic reaction of the same materials in refluxing acetonitrile produced the same products upon workup, however, at lower yields, suggesting that the redox chemistry in this experiment may be attributed to the serendipitous oxidation of Pd(0) or Pt(0) by impurities in the commercial elemental mercury, presumably HgO. The same reaction ($CH_3CN$) using freshly distilled Hg(0) produces deep-red solutions that show no phosphorus−mercury coupling by $^{31}$P{$^1$H} NMR spectroscopy, nor do they contain **1** or **2**. Both **1** and **2** can be prepared by reacting divalent $Pd(NCC_6H_5)_2Cl_2$ or Pt(1,5-cyclooctadiene)$Cl_2$ with $P_2$phen in the presence of freshly distilled Hg(0) in refluxing acetonitrile. Interestingly, the direct addition of $Hg_2(NO_3)_2$ to $P_2$phen and the appropriate $d^{10}$ metal starting material does not produce **1** or **2**.

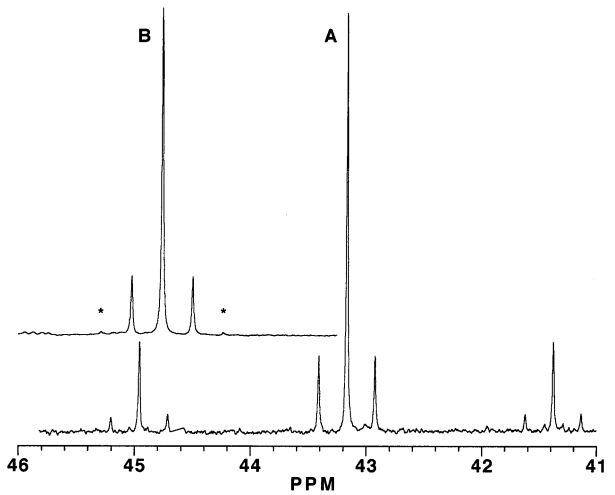


**Figure 1.** Downfield region of the 121.7 MHz $^{31}$P{$^1$H} NMR spectra of **1** (spectrum A) in $CD_3CN$ at 25 °C showing coupling to $^{195}$Pt ($I = 1/2$, 33.8% abundant) and $^{199}$Hg ($I = 1/2$, 16.8% abundant) and of **2** (spectrum B) showing coupling to $^{199}$Hg. Coupling to the isotopomer containing two $^{199}$Hg atoms (triplet, 2.8% abundant) is denoted by the asterisks.

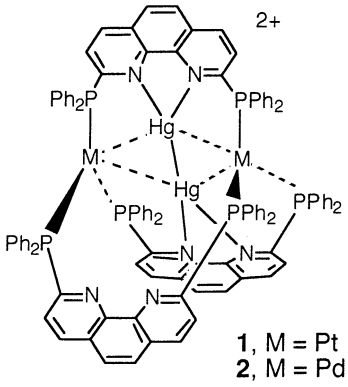


As shown in Figure 1, the $^{31}$P{$^1$H} NMR spectrum of **1** shows a single sharp resonance at 43.1 ppm for the phosphorus atoms of the $P_2$phen ligand with both $^{195}$Pt ($^1J_{P-Pt} = 4350$ Hz) and $^{199}$Hg ($^2J_{P-Hg} = 620$ Hz) satellites and the appropriate resonance for the $PF_6^-$ counterions at −143.5 ppm (heptet $^1J_{P-F} = 704$ Hz). Both $^{199}$Hg and $^{195}$Pt have $I = 1/2$ and are 16.8% and 33.8% naturally abundant, respectively. Simple integration of these resonances shows that the Hg satellites comprise approximately 34% of the total signal confirming the presence of two Hg atoms. Likewise, the overall 2+ charge is confirmed by comparison of the integration of the $PF_6^-$ signal and direct observation of two anions in the X-ray crystallography (vide infra). The

(15) *International Tables for X-ray Crystallography*; Kynoch Press: Birmingham, U.K., 1974; Vol. 4.

$^{31}P\{^{1}H\}$ NMR spectrum for **2** is similar to that of **1** with a single resonance for the $P_2$phen ligands at 44.9 ppm with $^{199}Hg$ satellites ($^{2}J_{P-Hg} = 638$ Hz). The observation of a single magnetic environment for the phosphorus atoms of the $P_2$phen ligands suggests that the $Hg_2^{2+}$ core is dynamic and is rapidly rotating about the Pt−Pt or Pd−Pd vectors at room temperature. Lowering the temperature to −90 °C broadens the $P_2$phen resonance of **1** and **2**, but no splitting is observed.

The 89.4 MHz $^{199}Hg$ NMR spectrum (vs $Hg(OAc)_2$ in $d_6$-DMSO) of **2** (Figure 2, top) shows the requisite heptet pattern at 833 ppm while for **1** a heptet (major isotopomer, no $^{195}Pt$ present) superimposed on a doublet of heptets (intermediate isotopomer, one $^{195}Pt$ present) is observed at 770.8 ppm (Figure 2, middle). Because of the low signal-to-noise of this spectrum, the outer lines of the doublet of heptets are not resolved nor is the minor isotopomer containing two $^{195}Pt$ atoms. Because of the large number of lines, the $^{199}Hg-^{195}Pt$ coupling is difficult to determine in this spectrum; however, this interaction is easily measured in the 106.9 MHz $^{195}Pt$ NMR spectrum (Figure 2, bottom) that displays a quartet at −3071 ppm with $^{199}Hg$ satellites and a $^{1}J_{Pt-Hg}$ value of 1602 Hz. The $^{1}H$ NMR spectra of **1** or **2** show only a single ligand environment with nine resonances easily assigned to the protons of the $P_2$phen ligands. As observed in other $P_2$phen-based metallocryptands, there are two environments for the phenyl rings, one axial and one equatorial to the $d^{10}-d^{10}$ metal−metal axis.

Crystals of **1** suitable for X-ray diffraction analysis were grown by the slow diffusion of benzene into a 1,2-dichloroethane solution of the complex and crystallize in the monoclinic space group $P2(1)/n$. The $PF_6^-$ salt of **2** did not produce satisfactory crystals; however, metathesis to the $BF_4^-$ salts produced deep-red, high quality crystals by slow diffusion of benzene into a 1,2-dichloroethane solution of the complex. **$2(BF_4)_2$** also crystallizes in the monoclinic space group $P2(1)/n$.

A thermal ellipsoid drawing of the cation of **1** is presented in Figure 3 while the cationic portion of **2** is shown in Figure 4. Selected bond distances and angles are presented in Table 2. The overall geometry of the complexes is helical; however, the bulk material is racemic as dictated by the centrosymmetric space group, and both helices are present. Both **1** and **2** contain a $Hg_2^{2+}$ unit coordinated to the phenanthroline portion of two $P_2$phen ligands and oriented nearly perpendicularly to the $d^{10}\cdots d^{10}$ metal−metal vector (Figure 5). The formal metal−metal bond of $Hg_2^{2+}$ moiety is evident with short Hg(1)−Hg(2) separations of 2.7362(6) and 2.6881(4) Å for **1** and **2**, respectively. The mercurous dimer interacts strongly and nearly symmetrically with the trigonally coordinated capping metals with Pt(1)−Hg(1), Pt(1)−Hg(2), Pt(2)−Hg(1), and Pt(2)−Hg(2) separations of 2.8045(5), 2.8258(6), 2.8447(6), and 2.7823(5) Å, respectively, and Hg(1)−Pt(1)−Hg(2) and Hg(1)−Pt(2)−Hg(2) angles of 58.152(13)° and 58.178(13)° in **1**. In **2**, the corresponding metrical parameters are very similar with Pd(1)−Hg(1), Pd(1)−Hg(2), Pd(2)−Hg(1), and Pd(2)−Hg(2) separations of 2.7936(6), 2.7475(5), 2.7419(5), and 2.7960(6) Å and

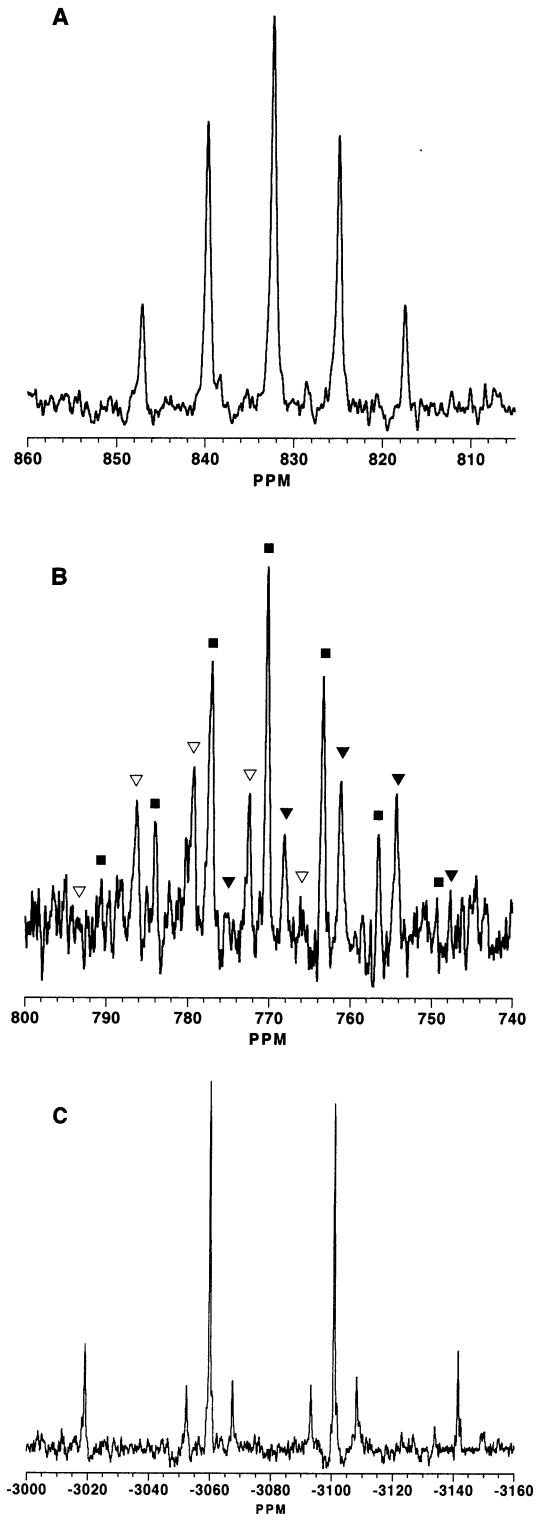


**Figure 2.** Spectrum A: the 89.4 MHz $^{199}Hg$ NMR spectrum (vs $Hg(OAc)_2$ in $d_6$-DMSO) of **2** shows coupling to six equivalent phosphorus atoms ($^{2}J_{P-Hg} = 638$ Hz). Spectrum B: the 89.4 MHz $^{199}Hg$ NMR spectrum of **1** displaying a heptet (■) for the non-$^{195}Pt$ containing isotopomer (43.8% naturally, abundant) and the inner lines of a doublet of heptets (△, ▲) for the isotopomer containing one $^{195}Pt$ atom (44.8% naturally abundant) with $^{2}J_{P-Hg} = 620$ Hz and $^{1}J_{Hg-Pt} = 1602$ Hz. The remaining isotopomer containing two $^{195}Pt$ atoms (11.4% naturally abundant) is not observed. Spectrum C: 106.9 MHz $^{195}Pt$ NMR spectrum of **1** showing coupling to three equivalent phosphorus atoms ($^{1}J_{Pt-P} = 4350$ Hz) and $^{199}Hg$ satellites ($^{1}J_{Pt-Hg} = 1602$ Hz).

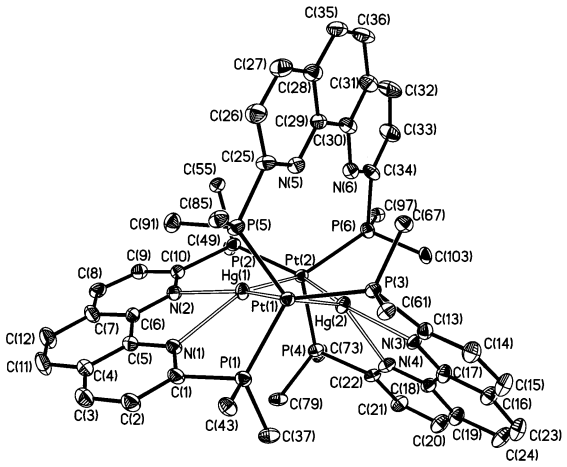


**Figure 3.** X-ray structural drawing for the cation of **1** viewed looking down the Pt−Pt axis. Hydrogen atoms and all but the ipso carbon of the phenyl rings omitted for clarity.

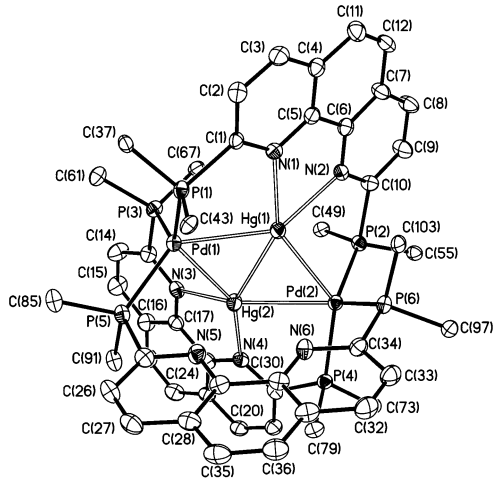


**Figure 4.** Thermal ellipsoid plot of the cationic portion of **2** with hydrogen atoms and all but the ipso carbon of the phenyl rings omitted for clarity. The axial phenyl rings are attached to C(37), C(61), C(85) on the left and to C(55), C(73), and C(97) on the right.

Hg(1)−Pd(1)−Hg(2) and Hg(1)−Pd(2)−Hg(2) angles of 58.035(11)° and 58.068(11)°, respectively.

In both complexes, the $d^{10}$ metal resides in a distorted trigonal coordination environment. In **1**, Pt(1) and Pt(2) are displaced out of their respective phosphine planes toward the $Hg_2^{2+}$ dimer by 0.563 and 0.587 Å, and in **2**, Pd(1) and Pd(2) are likewise displaced by 0.587 and 0.576 Å, respectively. These distortions shorten the Pt(1)···Pt(2) distance in **1** to 4.878(1) Å and the Pd(1)···Pd(2) distance to 4.806(1) Å in **2**. These values are considerably shorter than the P···P separations of the $P_2$phen ligands which average 6.771(3) Å in **1** and 6.805(3) Å in **2**. The short $d^{10}$···$d^{10}$ separations are achieved by twisting the two $PtP_3$ and $PdP_3$ units in the respective compounds. In **1**, the average intraligand torsion angle (P−Pt(1)−Pt(2)−P) is 87.2° while in **2** the analogous torsional angles are slightly larger with an average value of 91.4°.

The electronic absorption spectra ($CH_2Cl_2$) of **1** and **2** show broad, nearly featureless absorption bands that tail into the visible with shoulders discernible at 320 and 370 nm in **1** and 310 and 340 nm for **2**. Both show ligand-based $\pi-\pi^*$ transitions at 283 nm. The lowest energy band in **1** appears at 475 nm while in **2** this band is shifted to 430 nm. Excitation into these bands produces weak emissions centered at 593 nm with shoulders at 530 and 654 nm in **1** and centered at 524 nm with a shoulder at 545 nm in **2**. The excitation spectra show that these emissions are derived from the lowest energy absorption bands in the respective compounds. Neither **1** nor **2** demonstrated any reversible electrochemistry, nor was a molecular ion found in the

**Table 2.** Bond Distances (Å) and Angles (deg) for **1** and **2**

| | **1**, M = Pt | **2**, M = Pd |
|---|---|---|
| M(1)−Hg(1) | 2.8045(5) | 2.7936(6) |
| M(1)−Hg(2) | 2.8258(6) | 2.7475(5) |
| M(2)−Hg(1) | 2.8447(6) | 2.7419(5) |
| M(2)−Hg(2) | 2.7823(5) | 2.7960(5) |
| Hg(1)−Hg(2) | 2.7362(6) | 2.6881(4) |
| M(1)−P(1) | 2.3017(17) | 2.3304(15) |
| M(1)−P(3) | 2.2990(17) | 2.3644(16) |
| M(1)−P(5) | 2.3246(18) | 2.3633(17) |
| M(2)−P(2) | 2.3078(17) | 2.3611(16) |
| M(2)−P(4) | 2.3175(17) | 2.3379(16) |
| M(2)−P(6) | 2.3338(18) | 2.3730(16) |
| Hg(1)−N(1) | 2.468(5) | 2.344(5) |
| Hg(1)−N(2) | 2.398(5) | 2.453(5) |
| Hg(2)−N(3) | 2.401(5) | 2.483(5) |
| Hg(2)−N(4) | 2.500(5) | 2.360(5) |
| M···M | 4.878(1) | 4.806(1) |
| P(1)···P(2) | 6.758(3) | 6.779(2) |
| P(3)···P(4) | 6.776(3) | 6.781(2) |
| P(5)···P(6) | 6.779(3) | 6.854(2) |
| | **1**, M = Pt | **2**, M = Pd |
| P(1)−M(1)−P(3) | 120.20(6) | 120.67(6) |
| P(1)−M(1)−P(5) | 113.58(6) | 109.58(6) |
| P(3)−M(1)−P(5) | 108.84(6) | 111.57(6) |
| P(2)−M(2)−P(4) | 115.98(6) | 119.33(6) |
| P(2)−M(2)−P(6) | 115.26(6) | 113.85(6) |
| P(4)−M(2)−P(6) | 110.17(6) | 109.45(6) |
| M(1)−Hg(1)−Hg(2) | 61.313(15) | 60.124(12) |
| M(1)−Hg(2)−Hg(1) | 60.534(10) | 61.842(13) |
| Hg(1)−M(1)−Hg(2) | 58.152(13) | 58.035(11) |
| M(2)−Hg(1)−Hg(2) | 59.770(11) | 61.975(13) |
| M(2)−Hg(2)−Hg(1) | 62.052(13) | 59.957(12) |
| Hg(1)−M(2)−Hg(2) | 58.178(13) | 58.068(11) |
| N(1)−Hg(1)−N(2) | 67.44(19) | 68.95(17) |
| N(3)−Hg(2)−N(4) | 67.82(18) | 68.51(17) |
| P(1)−M(1)−M(2)−P(2) | 83.93(7) | 91.92(6) |
| P(3)−M(1)−M(2)−P(4) | 88.77(6) | 91.65(6) |
| P(5)−M(1)−M(2)−P(6) | 88.98(7) | 90.73(6) |

**Table 3.** Crystallographic Data for **1** and **2**

| | **$1(PF_6)_2\cdot1.5C_6H_6\cdot$ 1,2-$C_2H_4Cl_2$** | **$2(BF_4)_2\cdot0.5C_6H_6\cdot$ 0.75(1,2-$C_2H_4Cl_2$)** |
|---|---|---|
| formula | $C_{119}H_{90}Cl_2F_{12}$-$Hg_2N_6P_8Pt_2$ | $C_{112.5}H_{78}B_2Cl_{1.5}$-$F_8Hg_2N_6P_6Pd_2$ |
| fw | 2941.99 | 2540.40 |
| *a*, Å | 16.995(4) | 17.5937(18) |
| *b*, Å | 27.707(6) | 29.218(3) |
| *c*, Å | 23.561(5) | 19.122(2) |
| *β*, deg | 99.329(4) | 90.979(9) |
| *V*, Å$^3$ | 10948(4) | 9828.3(18) |
| space group | *P*2(1)/*n* | *P*2(1)/*n* |
| *Z* | 4 | 4 |
| $D_{calcd}$, g/cm$^3$ | 1.785 | 1.717 |
| cryst size, mm$^3$ | 0.16 × 0.23 × 0.34 | 0.13 × 0.13 × 0.32 |
| $\mu$ (Mo K$\alpha$), mm$^{-1}$ | 5.583 | 3.683 |
| $\lambda$, Å | 0.71073 | 0.71073 |
| temp, K | 135(2) | 143(2) |
| transm factors | 0.28−0.47 | 0.39−0.69 |
| R1, wR2 ($I > 2\sigma(I)$) | 0.0510, 0.1374 | 0.0490, 0.1182 |

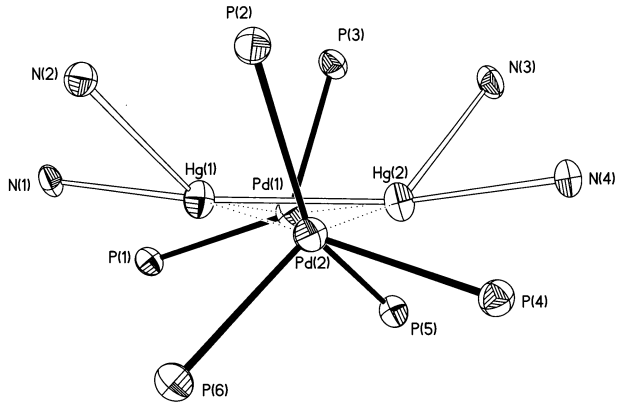


**Figure 5.** View of the coordination environment around the metals of **2**. The three $P_2$phen ligands are composed of P(1)−P(2), P(3)−P(4), and P(5)−P(6).

MALDI-TOF mass spectrum. However, several fragments corresponding to ligand dissociation and $Hg_2$ loss were discernible.

## Discussion

The redox chemistry leading to the formation of **1** and **2** is not completely understood but can be traced to either oxidative processes originating in the capping metals or to an impurity in the commercial grade mercury. It is well-known that the comproportionation equilibrium reaction of Hg(II) and Hg(0) strongly favors $Hg_2^{2+}$,[16] and this dimer is stabilized by nitrogen donor ligands such as $PhNH_2$ or 1,10-phenanthroline. The observations that **1** and **2** can be produced from either a legitimate Pt(II) or Pd(II) reagent or by the reaction of the zerovalent metals with $CH_2Cl_2$, producing Pt(II) or Pd(II) in situ, support the role of oxidative addition as a fundamental step in the synthesis. A subsequent transmetalation reaction or electron transfer with Hg(0) completes the final redox step to form $Hg_2^{2+}$. In the absence of a source of Pt(II) or Pd(II), an impurity, presumably HgO, in the commercial elemental mercury is needed to produce **1** and **2**. After purifying the mercury and eliminating sources of Pt(II) and Pd(II), no trace of either **1** or **2** could be found. It is interesting to note that the addition of $Hg_2(NO_3)_2$ to $Pd_2(dba)_3$ or $Pt(dba)_2$ in $CH_3CN$ does not produce **1** or **2** suggesting that a stepwise assembly of the metals may be necessary.

The dynamic behavior of the encapsulated $Hg_2^{2+}$ dimer is particularly striking especially when considering the large number of known stable and inert complexes of $Hg_2^{2+}$ with similar nitrogen-containing ligands including pyridine, 2,2′-bipyridine, and 1,10-phenanthroline.[17] To render the phosphine environments equal in the $^{31}P\{^1H\}$ NMR spectrum (likewise, the mercury environments) requires labilization of the Hg−N bonds and subsequent rotation of the $Hg_2^{2+}$ dimeric unit about the Pd···Pd or Pt···Pt axes. Assuming this mechanism is correct, Hg−N bond breaking is likely the rate-determining step, and considering that the Hg−N bond strengths are nearly the same for both compounds (average Hg−N separation is 2.442 Å in **1** and 2.410 Å in **2**), it is not unexpected that both complexes would exhibit similar dynamic behavior. Given the seemingly small barrier to rotation, variable temperature solid-state $^{31}P$ or $^{199}Hg$ NMR spectroscopy might be a better probe of this dynamic behavior. Clearly, further investigation is warranted.

Unlike other Pd(0)- and Pt(0)-based metallocryptands, the $^{31}P\{^1H\}$ NMR chemical shifts for **1** and **2** (43.1 and 44.9 ppm) are very similar. Typically, the $^{31}P$ resonances in Pd(0)-based metallocryptands are shifted 10−15 ppm upfield relative to their Pt(0) counterparts. Considering the large chemical shift dispersion of $^{199}Hg$ (>5000 ppm),[18] the $^{199}Hg$ resonances of **1** and **2** (770.8 and 833.0 ppm) are also considered very similar and close to the value for aqueous mercurous ion extrapolated to infinite dilution (∼800 ppm vs $Hg(OAc)_2$).[19] However, these resonances are shifted considerably downfield relative to the $^{199}Hg$ resonance observed in $[Au_2Hg(P_2phen)_3]^{2+}$ (−1200 ppm) which contains a single Hg(0) atom encapsulated in a Au(I)-cage.[7] The $^{195}Pt$ resonance of **1** (−3071 ppm) is significantly deshielded compared to the loosely related Tl(I)-containing metallocryptands, $[Pt_2Tl(P_2phen)_3]^+$(−4119 ppm) and $[Pt_2Tl(P_2bpy)_3]^+$ (−4120 ppm), and the archetypal $Pt(PPh_3)_3$ compound (−4583 ppm).[20] No analogous $^1J_{Pt-Hg}$ values for Pt(0) complexes bound side-on to a $Hg_2^{2+}$ unit could be found, but the $^1J_{Pt-Hg}$ of 1602 Hz observed in **1** is much smaller than the one-bond coupling constant of 5087 Hz found in $[N(CH_2CH_2PPh_2)_3Pt(HgMe)](BPh_4)$[21] which can be viewed as having a formal Pt−Hg bond.

The bonding about the four-metal center is unique, and no analogous compounds with two Pd or Pt atoms coordinated "side-on" to a mercurous dimer could be found. However, there are several triangular adducts of $Fe(CO)_4$ to mercurous dimer complexes that possess short Fe−Hg separations (∼2.55 Å) but with much longer Hg−Hg separations (∼3.1 Å)[17b,22] and numerous cluster compounds that contain Hg−Pt bonds[21,23] with separations ranging 2.531(1)−3.071(3) Å. It is notable in **1** and **2** that the Hg−

(16) Greenwood, N. N.; Earnshaw, A. *Chemistry of the Elements*; Pergamon Press: Oxford, 1994.

(17) (a) Kepert, D. L.; Taylor, D. *Aust. J. Chem.* **1974**, *27*, 1199−1202. (b) Mauro, A. E.; Pulcinelli, S. H.; Santos, R. H. A.; Gambardella, M. T. P. *Polyhedron* **1992**, *11*, 799−803. (c) Brodersen, K.; Hacke, N. *Chem. Ber.* **1974**, *107*, 3260−3265.

(18) Wrackmeyer, B.; Contreras, R. In *Annual Reports on NMR Spectroscopy*; Webb, G. A., Ed.; Academic Press: London, 1992; Vol. 24, p 267−329.

(19) Gillespie, R. J.; Granger, P.; Morgan, K. R.; Schrobligen, G. J. *Inorg. Chem.* **1984**, *23*, 887−891.

(20) Mann, B. E.; Musco, A. *J. Chem. Soc., Dalton Trans.* **1975**, 1673−1677.

(21) Ghilardi, C. A.; Midollini, S.; Moneti, S.; Orlandini, A.; Scapacci, G.; Dakternieks, D. *J. Chem. Soc., Chem. Commun.* **1989**, 1686−1688.

(22) (a) Baker, R. W.; Pauling, P. *J. Chem. Soc., Chem. Commun.* **1970**, 573−574. (b) Baird, H. W.; Dahl, L. F. *J. Organomet. Chem.* **1967**, *7*, 503−514.

(23) (a) Hao, L.; Manojlovic-Muir, L.; Muir, K. W.; Puddephatt, R. J.; Spivak, G. J.; Vittal, J. J.; Yufit, D. *Inorg. Chim. Acta* **1997**, *265*, 65−74. (b) Hao, L.; Vittal, J. J.; Puddephatt, R. J. *Organometallics* **1996**, *15*, 3115−3123. (c) Dahmen, K.-H.; Imhof, D.; Venzani, L. M.; Gerfin, T.; Gramlich, V. *J. Organomet. Chem.* **1995**, *486*, 37−43. (d) Spivak, G. J.; Vittal, J. J.; Puddephatt, R. J. *Inorg. Chem.* **1998**, *37*, 5474−5481. (e) Spivak, G. J.; Hao, L.; Vittal, J. J.; Puddephatt, R. J. *J. Am. Chem. Soc.* **1996**, *118*, 225−226. (f) Casas, J. M.; Falvello, L. R.; Forniés, J.; Gomez, J.; Rueda, A. *J. Organomet. Chem.* **2000**, *593−594*, 421−426.

Hg bond (2.7362(6) and 2.6881(4) Å) is preserved and is only slightly lengthened compared to the distance of 2.508(2) Å measured in $Hg_2(NO_3)_2$,[24] whereas the addition of $Fe(CO)_4$ to this core significantly weakens the Hg−Hg bond. The $Hg_2^{2+}$ unit strongly interacts with the $d^{10}$ metals as evidenced by the very short separations between the centroid of the $Hg_2^{2+}$ bond and Pd and Pt. In **1**, the $Hg_2$(centroid)−Pt(1) and Hg2(centroid)−Pt(2) separations are only 2.460 and 2.459 Å while in **2** the $Hg_2$(centroid)−Pd(1) and Hg2(centroid)−Pd(2) distances are slightly shorter at 2.423 and 2.421 Å. Considering these short separations and the rapid spinning of the $Hg_2^{2+}$ unit, it is tempting to draw an analogy between this interaction and that of the classic dihydrogen molecule bonded to a transition metal;[25] however, a better description might include a delocalized, four-centered molecular orbital approach that allows for strong Pt−Hg and Pd−Hg bonds without sacrificing the Hg−Hg bond. The average Pt−Hg bond length in **1** is 2.8143(6) Å while in **2** the average Pd−Hg bond length measures 2.7698(5) Å, and these values are in good agreement with other Pt−Hg[23] bonds and Pd−Hg bonds.[26]

The optical properties of **1** and **2** are consistent with those of other Pt(0)- and Pd(0)-based metallocryptands. For example, the deep-red, air-stable $[Pt_2Tl(P_2phen)_3]^+$ and $[Pd_2Tl(P_2phen)_3]^+$ are known to be very weakly emissive, and this emission likely originates from a metal-centered transition. Likewise, **1** and **2** exhibit very similar low-energy emissions that originate from allowed transitions that extend into the visible portion of the spectrum. The red shift of this absorption band in **1** compared to **2** also supports the assignment, and this trend was noted previously for analogous compounds.

Complexes **1** and **2** show for the first time the encapsulation of a molecular fragment rather than a single metal atom or ion suggesting that these metallocryptands could be used as templates for the synthesis of small multimetallic clusters. Clearly, there is room for another metal atom, and it is interesting that a third Hg atom is not trapped considering that the $Hg_3^{n+}$-polycations ($Hg_3(AlCl_4)_2$ and $Hg_3(AsF_6)_2$) are known.[16] Alternatively, it may also be possible to coordinate a different type of metal species to the vacant phenanthroline site in subsequent reactions. We are currently exploring this idea and the generation of similar clusters using other ligands.

**Acknowledgment** is made to the National Science Foundation (CHE-0091180), to the Donors of the Petroleum Research Fund, administered by the American Chemical Society, for their generous financial support of this research, and to Mr. Renante Yson for his assistance in preparing the graphical material.

**Supporting Information Available:** Complete X-ray crystallographic data for **1** and **2** (CIF format). This material is available free of charge via the Internet at http://pubs.acs.org.

IC020439N

(24) Grdenic, D.; Sikirica, M.; Vickovic, I. *Acta Crystallogr.* **1975**, *B31*, 2174−2175.
(25) Kubas, G. *Acc. Chem. Res.* **1988**, *21*, 120−128
(26) Bennett, M. A.; Contel, M.; Hockless, D. C. R.; Welling, L. L.; Willis, A. C. *Inorg. Chem.* **2002**, *41*, 844−855.
(27) Pauling, L. *The Chemical Bond*; Cornell University Press: Ithaca, NY, 1967.